Chemical Engineering Journal 475 (2023) 146282

Contents lists available at ScienceDirect

Chemical Engineering Journal

journal homepage: www.elsevier.com/locate/cej

Optimization of a combined system of vertical flow constructed wetland and solar photo-Fenton for ketoprofen removal in sewage and landfill leachate

Priscila Sabioni Cavalheri [a,b], Beatriz Santos Machado [b], Thalita Ferreira da Silva [a], João Pedro Baza Garcia Rodrigues [a], Fabio Gozzi [c], Fernando Jorge Correa Magalhães Filho [d], Rodrigo Pereira Cavalcante [e], Silvio César de Oliveira [a], Amilcar Machulek Junior [a,*]

[a] Institute of Chemistry, Federal University of Mato Grosso do Sul, Av. Senador Filinto Müller, 1555 Campo Grande, MS, Brazil
[b] Agrosantech-Agrotechnology-Oriented Sustainable Sanitation Research Group, Department of Sanitary and Environmental Engineering, Dom Bosco Catholic University, Av. Tamandaré, 6000 Campo Grande, MS, Brazil
[c] CMULTI-Multidisciplinary Center, Campus Floresta, Federal University of Acre, km 12, Cruzeiro do Sul, AC, Brazil
[d] Institute of Hydraulic Research, Federal University of Rio Grande do Sul, Av. Bento Gonçalves, 9500, Porto Alegre, RS, Brazil
[e] School of Technology, University of Campinas, Av. Paschoal Marmo, 1888 Limeira, SP, Brazil

ARTICLE INFO

Keywords:
Advanced oxidation processes
Pharmaceutical residue
Wastewater
Nature-based solutions
Toxicity
Design of experiments

ABSTRACT

Emerging contaminants in the environment are a matter of concern due to their widespread use and continuous disposal without proper treatment. Conventional treatments in sewage treatment plants (STPs) are not able to completely eliminate them, resulting in the presence of these compounds in several environmental matrices. Therefore, exploring and adding technologies to reduce or avoid the disposal of these compounds in the environment is necessary. This study aimed to use the solar photo-Fenton process combined with a partially saturated bottom vertical flow constructed wetland (VFCW) to remove ketoprofen (KET) from anaerobic effluent (sewage + landfill leachate) post-treated by a real-scale upflow anaerobic sludge blanket (UASB) reactor. The combined constructed wetland + solar photo-Fenton in pH 3.0 (CW + SPF3) and constructed wetland + solar photo-Fenton in pH 6.0 (CW + SPF6) systems showed high efficiency in degrading KET, achieving removal rates of 97% and 95%, respectively. The systems also showed efficiency in removing conventional parameters such as COD, $BOD_{5,20}$, and turbidity. In addition to having a lower cost, only the combined CW + SPF6 system was able to eliminate toxicity for Artemia sp. and Lactuca sativa (TU < 0.4). The solar photo-Fenton process and constructed wetlands have proven to be compatible technologies. This combination resulted in an innovative and effective method for wastewater treatment systems containing emerging contaminants. The use of new technological arrangements for the treatment of sewage and effluents, such as constructed wetlands (CWs), which are nature-based solutions, and environmentally sustainable advanced solar oxidation processes, establish a NEXUS concept, promoting the circular economy.

1. Introduction

Due to advances in the development of more sensitive analytical techniques, emerging contaminants, such as pesticides, microplastics, pharmaceutically active compounds, personal care products, and endocrine disruptors, among others, have been detected in air, soil, and water, usually at concentrations in the nanograms per liter (ng L^{-1}) range [1]. Improper disposal of these contaminants, especially pharmaceutically active compounds, poses a risk to the ecosystem even at low concentrations due to their mutagenic and carcinogenic potential [2,3]. Ketoprofen is a widely used drug in the treatment of rheumatoid arthritis and pain relief. Its presence in sewage treatment plants (STPs) has been detected at concentrations of 1000 ng/L [4,5].

The main ingress of emerging contaminants into the environment occurs through the discharge of wastewater effluents from sewage treatment plants (STPs) [6], as they cannot remove these micropollutants. Therefore, the use of new technological arrangements for sewage and effluent treatment, such as constructed wetlands (CWs),

* Corresponding author.
E-mail addresses: machulekjr@gmail.com, amilcar.junior@ufms.b (A.M. Junior).

https://doi.org/10.1016/j.cej.2023.146282
Received 12 July 2023; Received in revised form 25 August 2023; Accepted 24 September 2023
Available online 28 September 2023

which are nature-based solutions (NbS), and advanced oxidation processes (AOPs) is necessary as a complementary treatment to the commonly used technologies that do not have such capacity [7,8].

CWs and AOPs are usually investigated separately as processes for the removal of contaminants in STP effluents [9,10]. CWs are used to remove contaminants such as organic matter and nutrients through biological processes [11–13], while AOPs are advanced, non-selective technologies used to degrade and mineralize organic compounds resulting in smaller molecules, via free radicals, such as hydroxyl (HO•) [14–16]. A combined system of CWs and AOPs aiming for the treatment of urban wastewater would allow the use of both systems advantages for more efficient and complete pollution control. CWs have high efficiency in removing solids, turbidity, and organic matter [17,18], facilitating the absorption of solar irradiation by AOPs in the removal of emerging pollutants [19,20].

Although there are still no studies on CW + AOP in a real scale, a pilot-scale study that used a combined process of biological filtration and ozonation demonstrated high performance in the removal of conventional contaminants, with chemical oxygen demand (27.8 mg L^{-1}) and total nitrogen (9.9 mg L^{-1}) concentrations in the final effluent in compliance with local legislation limits (Beijing, China) for water reuse [21]. A study in 2020 [22] used a combination of horizontal flow constructed wetlands (HFCW), on a laboratory scale, and advanced oxidation processes (AOPs) to investigate the removal of some pharmaceutical compounds and found that the highest removal efficiency of the contaminants diclofenac (DCF) (90%) and carbamazepine (CBZ) (85%) was obtained when HFCW and solar photo-Fenton process (SPF) were studied as combined systems.

A combination of natural technologies and advanced treatment processes can provide a valuable alternative for the removal of micropollutants. However, there are still no consolidated studies on the use of partially saturated flow constructed wetlands combined with the solar photo-Fenton process. This is a newer variation of a NbS especially with integrated monitoring of physicochemical analyses, emerging contaminants, and ecotoxicity. NBSs, like CWs, combined with advanced technologies such as AOPs, can be promising for treatment aiming for effluent with quality and safe reuse, including the recovery of resources, especially nutrients.

The SPF process stands out among AOPs, as they are efficient for the oxidation of emerging contaminants (ECs), and environmentally sustainable. The oxidation efficiency of the system is enhanced by the extra generation of HO• from the photolytic reduction of the $Fe(OH)^{2+}$ complex to Fe^{2+} (Eq. (1)) [23,24]. The Fe^{3+}/Fe^{2+} catalytic cycle is improved by the photolysis of Fe^{3+} complexes with carboxylate intermediates (Eq. (2)) [25,26]. Then, Fe^{2+} reacts with H_2O_2 producing Fe^{3+}, OH^-, and HO•, closing the catalytic cycle (Eq. (3)). The process has been widely studied at the optimum pH for the photo-Fenton reaction (pH 2.5–3.0) [27–30], however, the low pH makes the reuse or even proper environmental disposal in nature (soil or water) unfeasible.

$$Fe(OH)^{2+} + h\nu \rightarrow Fe^{2+} + HO^{\bullet} \quad (1)$$

$$Fe(OOCR)^{2+} + h\nu \rightarrow Fe^{2+} + CO_2 + R^{\bullet} \quad (2)$$

$$Fe^{2+} + H_2O_2 \rightarrow Fe^{3+} + OH^- + HO^{\bullet} \quad (3)$$

Studies have been advancing in neutral pH treatment to overcome the costs associated with large-scale acidification and neutralization [31,32]. One possibility to overcome this disadvantage is the use of biodegradable and non-toxic organic ligands of low molar mass that form complexes with iron (Eq. (4)), increasing the operating pH range to almost neutral [33,34].

$$[Fe^{3+}.\ L] + h\nu \rightarrow [Fe^{3+}.\ L]^* \rightarrow Fe^{2+} + L^* \quad (4)$$

Therefore, the use of chelating agents that prevent the precipitation of iron, in the form of $Fe(OH)_3$, at nearly neutral pH, has been gaining increasing attention and, among them, citrate (Cit) stands out. Citrate is biodegradable, can be reused from waste originating from natural products, and its use is considered safe for the environment [35,36].

The use of these advanced processes may result in the generation of toxic and/or more toxic compounds than the initial samples [37,38]. Therefore, in addition to the evaluation of routinely investigated physicochemical parameters, ecotoxicological analyses should be performed [39]. When investigating the elimination of toxicity, complete mineralization is not necessary, which consequently reduces the costs of applying these processes on a real scale.

In this work, the main novelty is in the use of a combined system of vertical flow constructed wetlands and solar photo-Fenton process at optimal pH (3.0) (CW + SPF3) and near neutral pH (6.0) (CW + SPF6) for the degradation of ketoprofen and mineralization of organic matter in real-scale wastewater treatment plant effluent. Design of experiments and a compound parabolic collector (CPC) as a solar photoreactor were used. The physicochemical parameters and toxicity in Artemia sp. and Lactuca sativa were evaluated in the treated effluents.

2. Materials and methods

2.1. Study location and effluent sampling

The effluent was collected from the outlet of a vertical flow constructed wetland (VFCW) that receives effluent from the upflow anaerobic sludge blanket (UASB) reactors at the Los Angeles sewage treatment plant (STP), located in the city of Campo Grande, capital of the state of Mato Grosso do Sul, Brazil, with latitude 20°39′27.27″S and longitude 54°50′52.36″W. The main treatment at STP Los Angeles consists of 10 UASB reactors with an operating capacity of 1100 L s^{-1}, responsible for treating about 90% of the effluent generated by the municipality, including drainage and sewage, as well as leachate produced by the municipal landfill with an average flow rate of 5.05 L s^{-1}, corresponding, throughout the day, to 1.0% of the total effluent. The treated effluent is released into the Anhanduí river (classification IV;[40]).

Ketoprofen (KET; 25 mg L^{-1}) was added to the inflow of the VFCW, mixed in a reservoir, with the volume of one pulse (±190 L), plus the dead volume below the suction pump (±110 L), totaling 300 L. The amount of the drug in mg L^{-1} was added to allow the study of degradation and mineralization, due to the detection limit of the technique used, such as Total Organic Carbon analyzer (TOC) and High-Performance Liquid Chromatography (HPLC).

After 7.2 h (0.3 days) from the start of feeding, the effluent was collected and stored at 4 °C. The experiments in the solar reactor were conducted from 11 a.m. to 1p.m. (the period with the highest solar incidence) at the Federal University of Mato Grosso do Sul, Brazil (latitude 20°50′57.54″S and longitude 54°61′72.21″W). The graphical summary of the procedures performed is shown in Fig. 1.

The average annual temperature was 24.5 °C, with a relative humidity of 69%, and tropical climate, with sun throughout the period.

2.2. Physicochemical characterization of effluents

Physical and chemical analyses were carried out according to the methods and techniques described in the Standard Methods for the Examination of Water and Wastewater [41]. The physicochemical characteristics of the effluents are summarized in Table 1.

2.3. Partially saturated vertical flow constructed wetlands operational conditions

The vertical flow constructed wetland (VFCW) was planted with *Typha domingensis*, with a surface area of 12 m^2 and a total height of 85 cm, with the last 40 cm saturated with sewage. The filtering medium consisted of 40 cm of sand, with a free surface layer of 5 cm for application of the effluent and prevention of overflow due to possible clogging, a layer of 25 cm of gravel (5 to 10 mm) on the surface to prevent

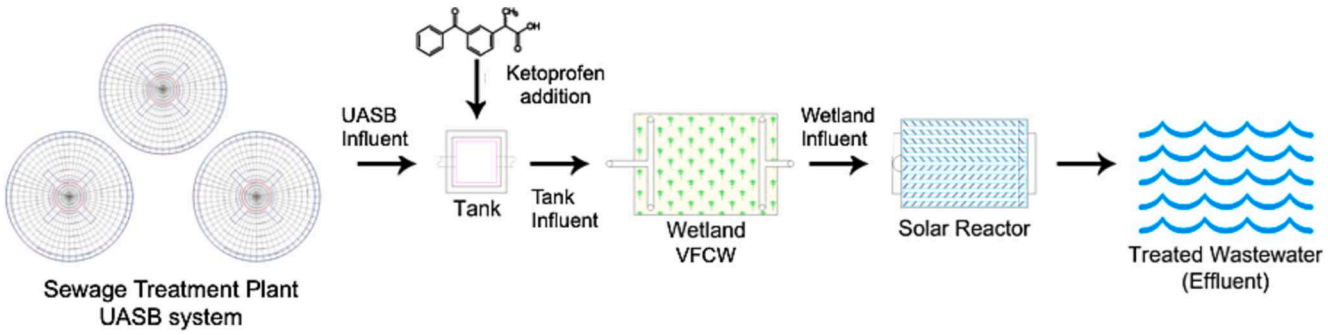

Fig. 1. Graphic scheme of the combined CW + AOP system (Solar Reactor).

Table 1
Physicochemical characteristics of the effluents studied.

Parameters	Raw Sewage	SW	VFCW	Release limits standard**	Methods
Temperature (°C)	26.6 ± 4.4	27.2 ± 4.4	27.9 ± 3.9	< 40 °C	–
pH	7.4 ± 0.1	7.0 ± 0.2	6.4 ± 0.4	6.0 – 9.0	4500B
Turbidity (NTU)	117.5 ± 17.08	28.5 ± 12.0	4.9 ± 1.8	–	2130B
TOC (mg L^{-1})	181.65 ± 0.34	127.35 ± 0.43	58.94 ± 0.92	–	NPOC
COD (mg L^{-1})	754.6 ± 59.73	338.5 ± 8.0	84.3 ± 42.3	–	5220B
BOD (mg L^{-1})	333.8 ± 30.78	68.9 ± 40.0	20.3 ± 3.3	< 120	5210B
TN (mg L^{-1})	127.7 ± 15.87	21.1 ± 3.2	3.9 ± 2.3	–	4500C
NO_2^- (mg L^{-1})	0.023 ± 0.005	2.4 ± 1.3	2.3 ± 2.4	–	4500B
NO_3^- (mg L^{-1})	2.0 ± 0.25	2.8 ± 0.8	4.5 ± 1.2	–	4110B
N-NH_4^+ (mg L^{-1})	76.0 ± 5.14	4.4 ± 1.2	2.4 ± 1.3	20	4500B and C
TP (mg L^{-1})	7.9 ± 0.79	4.4 ± 0.9	1.0 ± 0.5	–	4500 B5 and 4500 E
TS (mg L^{-1})	756.8 ± 120.06	674.0 ± 122.7	550.1 ± 92.1	–	2540B
Fe (mg L^{-1})	2.8 ± 0.006	1.3 ± 0.002	0.28 ± 0.06	15	3030 E and 3111B

*n = 14 samples; (±) standard deviation; Raw Sewage = UASB reactor inlet effluent; SW = UASB post-reactor effluent; TOC = Total organic carbon; COD = Chemical Oxygen Demand; BOD = Biochemical oxygen demand; TN = total nitrogen; N-NH_4 = ammonium nitrogen; TP = total phosphorus; TS = total solids; NPOC = non-purgeable organic carbon;
**Release limit values in class IV river [40]. There are no limits for turbidity, TOC, COD, TN, NO_2^-, NO_3^-, TP and TS in Brazilian legislation for class IV rivers.

erosion, and 20 cm of gravel (5 to 10 mm) at the bottom, operating in a downward flow, hydraulic loading of 128 mm d^{-1}, 8.8 (±5.1) gBOD m^{-2} d^{-1}, and 43.3 (±1.0) gCOD m^{-2} d^{-1} of post-treated sewage from the UASB reactor of the sewage treatment plant (STP).

2.4. Hydrodynamic characterization of partially saturated bottom vertical flow constructed wetland (VFCW)

2.4.1. Tracer test

The objective of the tracer test was to verify the behavior of fluids in the VFCW and find the peak time (pt) of the tracer. The pt corresponds to the time of collection at which there would be the highest concentration of the ketoprofen (KET) drug in the constructed wetland (CW) effluent. To read the salt concentration in the effluent (Fig. A1, see Supplementary material), a conductivity meter (Instrutherm mod. CD-850 Portable Digital) was used. The detailed procedure is described in the Supplementary Material and was carried out as described in [42–44].

2.5. Solid-phase extraction (SPE)

Samples of raw effluent, effluent from the vertical flow constructed wetland (VFCW), KET standard solution, and blank ultra-pure water (purified water in a reverse osmosis system with a resistivity<18.2 MΩ cm (Gehaka, São Paulo, Brazil) were eluted in Strata C18-E cartridges (55 µm, 70A; 500 mg/6mL; Phenomenex), as described in [45]. The cartridges were connected to a Manifold vacuum system (Phenomenex), the tests were performed in triplicate, and the samples obtained were analyzed by high-performance liquid chromatography (HPLC).

2.6. KET degradation procedures by combined constructed wetland and solar photo-Fenton process (CW + SPF)

8L of vertical flow constructed wetland (VFCW) effluent (Fig. 2a) containing H_2O_2 and Fe^{2+} ($FeSO_4{\cdot}7H_2O$) at pH 3.0 (CW + SPF3) and/or H_2O_2/Fe^{3+}/Sodium citrate at pH 6.0 (CW + SPF6), was pumped from a 20L reservoir tank into borosilicate tubes (internal diameter 28 mm, length 851 mm, thickness 4 mm, with a total illuminated area of 0.2248 m^2) of the solar reactor (Fig. 2b). The reactor was oriented with a 15° inclination towards the east and continuously recirculated by a recirculation pump (Dancor, CP-4R, 1/4 hp M) operating at a constant flow rate of 180 L min^{-1}, determined using a flow meter, for a duration of 120 min [46,47]. The ferric citrate complex was formed in situ by adding sodium citrate ($Na_3C_6H_5O_7$) to the effluent, followed by the addition of ferric chloride [14]. The quantities of H_2O_2, Fe^{2+}/Fe^{3+}, and sodium citrate varied according to Table A1 and Table A2 (see Supplementary Material). In all experiments, the initial pH was adjusted with H_2SO_4 (0.1 mol/L) when necessary, and H_2O_2 (30% v/v) was added only at the beginning of the procedures. The temperature was kept below 35 °C in all experiments. The accumulated energy (Q_{uv}) was calculated (equation A.1, see Supplementary Material) [48], and the solar radiation dose (SRD) was measured during the experiments using a digital lux meter (AKSO, AK310) and converted to W m^{-2} with an appropriate conversion factor (1 Lux = 0.0079 W m^{-2}) [49,50].

After treatment, the samples were evaluated for physicochemical parameters, toxicity, total organic carbon (TOC), and KET concentration decay by HPLC. Immediately after each assay, the residual H_2O_2 concentration was measured using peroxide analytical test strips (Colorimetric Test Strips Method, 1–25 mg L^{-1}, Merck), and the concentration was<0.5 mg L^{-1} in all experiments.

2.7. Experiment optimization using Statistical design of experiments

For the removal of KET in the vertical flow constructed wetland (VFCW) effluent by solar photo-Fenton process at pH 3.0, a central composite design (CCD) with two axial points and a central point was applied to investigate the variables that influenced KET degradation and organic matter mineralization. Therefore, the concentration of H_2O_2 and

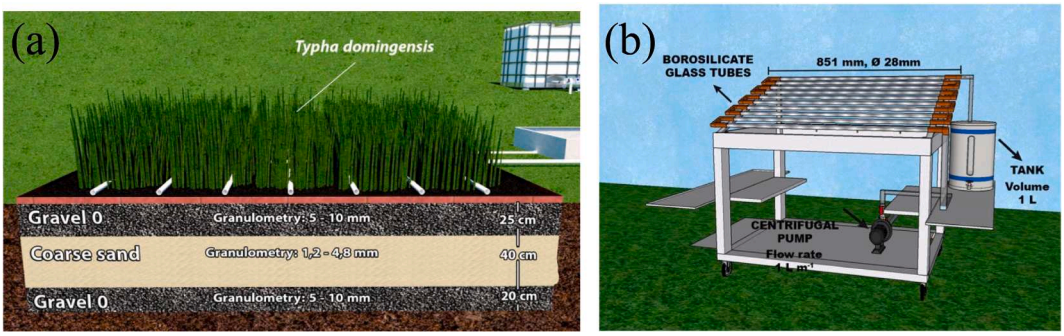

Fig. 2. Schematic representation of the Constructed Wetland (a) and the Solar Reactor (b) used in the experiments.

Fe^{2+} ions were chosen as independent variables (Table A1, see Supplementary Material), with a solar irradiation time of 120 min. Eleven experiments with triplicates at the central point were randomly generated using Statistica StatSoft software version 10. The range of limits applied for the two studied variables was chosen based on previous laboratory tests.

After optimizing the Fe^{2+} and H_2O_2 variables, a second experimental design model was applied using a 2^2 factorial design with the addition of a central point. The Fe^{3+}:Citrate ratio and the H_2O_2 concentration were selected as independent variables (Table A2, see Supplementary Material), and the pH was adjusted to 6.0. The significance of each model was identified using the p-value ($p < 0.05$). Statistical validation was obtained through analysis of variance (ANOVA) with a confidence level of 95%.

2.8. Acute toxicity assays

2.8.1. Lactuca sativa

Untreated Lactuca sativa seeds (cultivar Aurelia; 95% germination rate; Topseed brand; Lot no. 065044) were used for phytotoxicity assays. The assay was conducted following [51,52], and detailed procedures are described in the Supplementary Material.

2.8.2. Artemia sp

The acute ecotoxicity assay was performed according to the ABNT NBR 16530:2016 Brazilian standard. The results were expressed in toxic unit (TU) [53]. The ecotoxicity tests are described in detail in the Supplementary Material.

3. Results and discussion

3.1. Experimental design and optimization studies

3.1.1. Central composite design (CCD) for the combined constructed wetlands and solar photo-Fenton at pH 3.0 (CW + SPF3)

A CCD 2^2 with triplicates at the central point was applied to determine the influence of variables and experimental conditions that most affect the degradation of ketoprofen in the combined CW + SPF3 process.

The central points (20.00 mg L^{-1} of H_2O_2 and 9.00 mg L^{-1} of Fe^{2+}) (Table A3, see Supplementary Material) exhibited the best reaction conditions, achieving higher mineralization removal (35.9 ± 1.3%) and degradation rates (96.7 ± 0.64%) for the combined CW + SPF3 system within 120 min of the experiment, with solar radiation dose of $SRD_{UV} = 58.20\ W\ m^{-2}$, consuming accumulated energy of $Q_{uv} = 3.8\ kJ_{uv}\ L^{-1}$, at a 95% significance level.

Critical values for reaction optimization were calculated using Statistica 10 software, generating the following values: 22.58 mg L^{-1} of H_2O_2 and 9.61 mg L^{-1} of Fe^{2+} for the % mineralization, and 24.72 mg L^{-1} of H_2O_2 and 10.44 mg L^{-1} of Fe^{2+} for the % degradation. These values are very close to the values used in this work for the central points, indicating a good fit of the mathematical model to the experimentally used variable concentrations.

When comparing assay 6 with the central points (Table A3, see Supplementary Material), it is observed that increasing the H_2O_2 concentration leads to a decrease in the % degradation and % mineralization. This indicates that there is a limit to the increase of the oxidant concentration to prevent the recombination of hydroxyl radicals due to an excess of hydrogen peroxide.

Excessive peroxide can generate competitive reactions that produce an inhibitory effect on degradation. High concentrations of H_2O_2 can react with $HO^{\bullet}$ and form the weaker oxidants, HO_2 and $O_2^{\bullet}$. The $HO_2^{\bullet}$ that was produced react with $HO^{\bullet}$ and form water and oxygen and dimerized to H_2O_2 [54]. The $HO^{\bullet}$ radicals are prone to recombine or react according to Eqs. (5)–(8):

$$HO^{\bullet} + H_2O_2 \rightarrow HO_2^{\bullet} + H_2O \quad (5)$$

$$HO_2^{\bullet} + H_2O_2 \rightarrow HO^{\bullet} + H_2O + O_2 \quad (6)$$

$$2HO_2^{\bullet} \rightarrow H_2O_2 + O_2 \quad (7)$$

$$HO_2^{\bullet} + HO^{\bullet} \rightarrow H_2O_2 + O_2 \quad (8)$$

Reactions (5) and (8) consume $HO^{\bullet}$ and decrease the oxidation probability. It is important to determine the optimal amount of H_2O_2 to avoid an excess that may influence the degradation efficiency.

In Fig. 3a, the quadratic variables (Q): $[Fe^{2+}]$ and $[H_2O_2]$, and the linear variable (L): $[H_2O_2]$, were statistically significant ($p < 0.05$). This indicates that the process optimization is strongly dependent on these variables. In this model, the values of Fe^{2+} and H_2O_2 are negative, indicating that mineralization is favored at lower concentrations of these variables.

The observed values (blue dots) and the predicted values (red solid line) are presented in Fig. 3b and 5b for the responses: % mineralization ($R^2 = 0.9492$ and adjusted $R^2 = 0.8984$) and % KET degradation ($R^2 = 0.9768$ and adjusted $R^2 = 0.9535$), respectively. The observed values are close to the linear behavior. The adjusted R^2 value of the model is close to the observed R^2 value for both responses, indicating that the model was statistically satisfactory [55,56].

The empirical mathematical models for the efficiency of % mineralization (%MIN) (Eq. (9)) and % degradation (%DEG) (Eq. (10)) were generated based on the estimated regression coefficients, considering the variables and their mutual relationships.

$$\%\mathbf{MIN} = 46.66 + 4.23*[Fe^{2+}] - 0.09*[Fe^{2+}]^2 + 7.40*[H_2O_2] - 0.38*[H_2O_2]^2 - 0.002*[Fe^{2+}]*[H_2O_2]. \quad (9)$$

$$\%\mathbf{DEG} = 61.55 + 8.65*[Fe^{2+}] - 0.21*[Fe^{2+}]^2 + 10.79*[H_2O_2] - 0.70*[H_2O_2]^2 + 0.16*[Fe^{2+}]*[H_2O_2]. \quad (10)$$

To enhance the understanding of the behavior of the significant variables, three-dimensional response surface graphs (Fig. 4a) and contour graphs (Fig. 4b) were generated between the variables $[H_2O_2]$ and $[Fe^{2+}]$. It can be observed that when using about 20 mg L^{-1} of

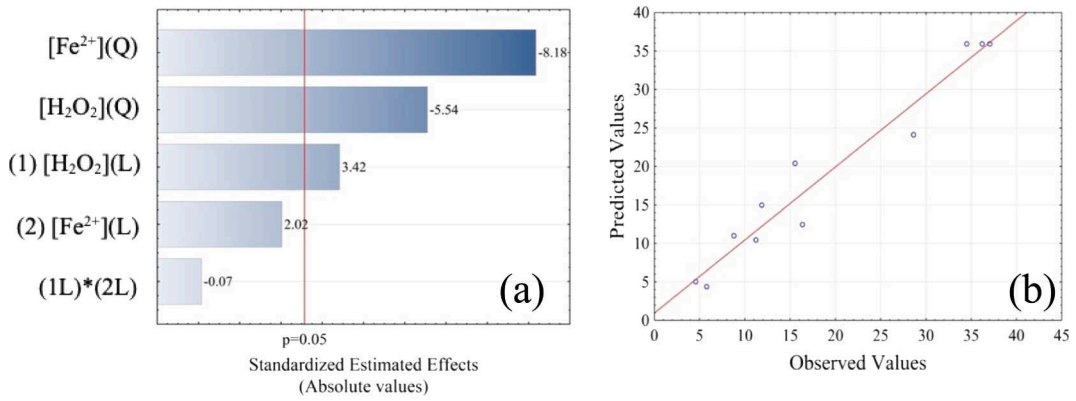

Fig. 3. Pareto chart (a) and Predicted versus observed values (b) for the effects of each variable on their interactions in relation to the percentage mineralization response of the CW + SPF3 process.

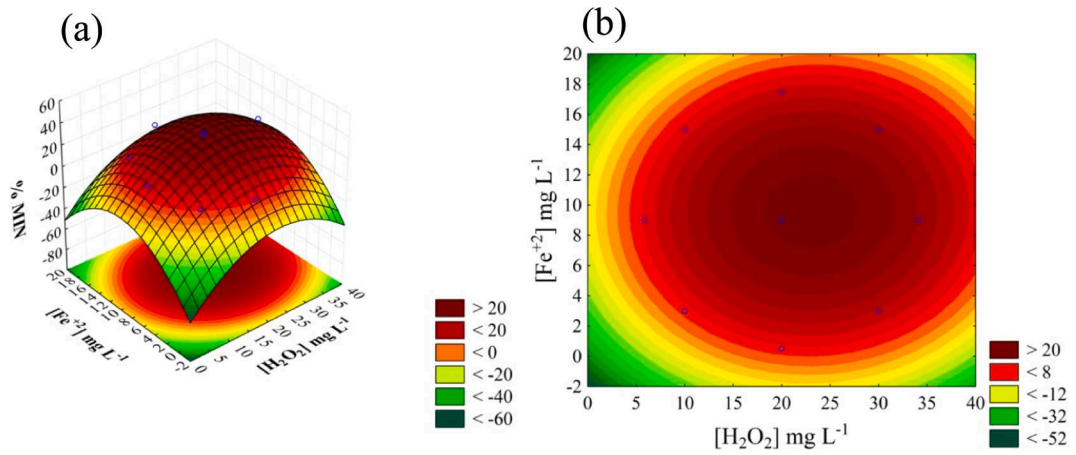

Fig. 4. Response surface graph (a) and contour curve (b) of the effects of each variable and their interactions on the percentage of mineralization response.

$[H_2O_2]$, a maximum of 8 to 10 mg L^{-1} of Fe^{2+} is necessary. As the concentration of Fe^{2+} or H_2O_2 is increased or decreased, there is a decrease in % mineralization. This effect of increasing concentrations may be related to competitive reactions that consume the HO• radical, which is primarily responsible for the oxidation of organic molecules [57,58]. In Fig. 4a and 4b, it was observed that the experimental points (blue dots) fell within the region of higher % mineralization (red region), indicating that the experiments were adequate in this model.

Domestic wastewater is a complex matrix containing Cl^-, NO_3^-, NO_2^-, CO_3^{2-}, and HCO_3^- ions, among others. Like Cl^-, NO_3^- and NO_2^- eliminate hydroxyl radicals from the solution, decreasing the efficiency of the process (Eqs. (11) and (12)).

$$HO^{\cdot} + Cl^- \rightleftarrows ClOH^{\cdot -} \rightleftarrows Cl^{\cdot} + HO^- \quad (11)$$

$$ClOH^{\cdot -} + H^+ \rightleftarrows ClOH_2^{\cdot} \rightleftarrows Cl^{\cdot} + H_2O \quad (12)$$

These species can interfere with the efficiency of the process by initiating chain reactions with H_2O_2, which occurs through the recombination of hydroxyl radicals (Eqs. (5)–(8)) [59,60].

For KET degradation in the effluent, all quadratic (Q) and linear (L)

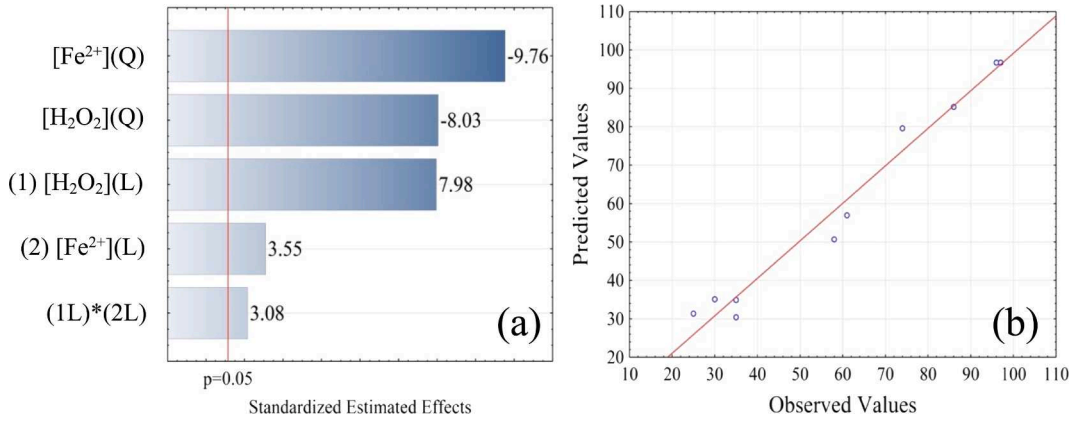

Fig. 5. Pareto chart (a) and Predicted vs. Observed values (b) of the variables' effects and their interactions on KET degradation.

variables, namely [Fe^{2+}] and [H_2O_2], as well as the interaction between Fe^{2+} and H_2O_2, were statistically significant ($p < 0.05$) (Fig. 5), indicating that all variables should be considered in the treatment optimization.

In Fig. 6a and 6b, the response surface graphs, and contour curve are presented, respectively, constructed from the interaction between the variables [Fe^{2+}] and [H_2O_2]. It is possible to observe the interaction and inhibitory effect as the concentrations of Fe^{2+} and H_2O_2 increase or decrease. The interaction between Fe^{2+} and H_2O_2 exhibited a synergistic behavior for the percentage degradation of KET. It was also observed that there is a limit to the increase in hydrogen peroxide concentration, as increasing the concentration above 20 mg L^{-1} results in a decrease in the percentage degradation, as seen in experiment 6 (Table A3, see Supplementary Material).

Similarly, by keeping the H_2O_2 concentration at 20 mg L^{-1} and increasing the Fe^{2+} concentration, both the percentage of mineralization and of degradation decrease. This indicates that the degradation and mineralization rates are highly dependent on the concentrations of Fe^{2+} and H_2O_2 [59,61], which are increased up to an optimal value, especially due to the formation of HO• radicals. However, any further increase may lead to a reduction in the efficiency of KET mineralization and degradation due to secondary reactions that consume the HO• radicals. Higher doses of hydrogen peroxide have an inhibitory effect on KET degradation.

3.1.2. *Factorial experimental design for the combined constructed wetlands and solar photo-Fenton system at pH 6.0 (CW + SPF6)*

After optimizing the Fe^{2+} and H_2O_2 variables obtained from the previous CCD at pH 3.0, a new 2^2 factorial experimental design with triplicate at the central point was performed for the combined CW + SPF6 process. With a solar radiation dose of $SRD_{UV} = 56.97 \pm 1.66$ W m^{-2}, the process consumed an average accumulated energy of $Q_{uv} = 3.69 \pm 0.11$ kJ_{uv} L^{-1}, where the 1:3 ratio of [Fe^{3+}:Citrate] complex showed high KET degradation efficiency (95 ± 0.20%) and organic matter mineralization (39.0 ± 0.65%) (experiment 4, Table A4, see Supplementary Material).

A pareto chart was built for mineralization (Fig. 7a). The [Fe^{3+}:Citrate] ratio was the most statistically significant variable, and the interaction between H_2O_2 and [Fe^{3+}:Citrate] was considered significant ($p < 0.05$).

In Fig. 7a, the significant interaction [Fe^{3+}:Citrate] × H_2O_2 showed synergy between the variables. This effect can be observed in experiment 4 (Table A4, see Supplementary Material), where higher values of these variables resulted in a higher percentage of mineralization. The opposite effect can be observed in experiments 2 and 3, where a decrease in the value of one of these variables led to a decrease in the percentage of mineralization.

Fig. 7b presents the plot of predicted values versus observed values. The blue points represent the experimental data, which closely follow the trend of the predicted values and are close to the red line. This indicates that the experiments were well fitted to the mathematical model, with $R^2 = 0.9929$ and adjusted $R^2 = 0.9859$.

Therefore, in order to predict the response functions for the percentage of mineralization (%MIN) and degradation (%DEG), the following Eqs. (13) and (14), respectively, were generated from the estimated regression coefficients, considering the variables and their mutual relationships.

$$\%\mathbf{MIN} = 5.81 + 6.42*[\text{Fe:Citrate}] - 0.50*[H_2O_2] + 0.32*[\text{Fe:Citrate}]*[H_2O_2] \quad (13)$$

$$\%\mathbf{DEG} = 38.35 + 14.05*[\text{Fe:Citrate}] - 0.56*[H_2O_2] + 0.36*[\text{Fe:Citrate}]*[H_2O_2] \quad (14)$$

In Fig. 8a and 8b, the three-dimensional response surface and contour graphs are presented, respectively, showing the interactions between the variables [H_2O_2] and [Fe^{3+}: citrate]. It can be observed that increasing the Fe^{3+}:Citrate ratio significantly increases the percentage of mineralization. This effect is attributed to the reaction between H_2O_2 and the ferric citrate complex, as well as the pH of the solution, where the amounts of H_2O_2 and the Fe^{3+}:Citrate ratios determine the concentration of reactive oxygen species in aqueous solutions, therefore affecting the photodegradation of compounds [62].

In Fig. 9a, the Pareto chart for the percentage degradation response variable, all variables were important for the process, but the Fe^{3+}:Citrate ratio was the most significant one. The ferric complex enables the reaction at near-neutral pH due to its higher quantum yield of Fe^{2+} generation ($\Phi Fe^{2+} = 0.28$ at 366 nm for Fe^{3+}: citrate) [32], which promotes the consumption of H_2O_2, generating HO• radicals more rapidly.

In Fig. 9b, the graph of predicted values versus observed values is presented. The blue points represent the experimental data and follow the trend of the predicted values, closely aligning with the red line. This indicates that the experiments are well-fitted to the mathematical model, with an R^2 of 0.9987 and an adjusted R^2 of 0.9974. The Fe^{3+}:Citrate ratio was also the most statistically significant independent variable. All variables showed positive values, indicating that the degradation percentage is favored by increasing their concentrations. There was a synergistic effect observed in the significant interaction between Fe^{3+}:Citrate and H_2O_2 (Fig. 10).

The degradation of KET through the CW + SPF6 process significantly decreased when Fe^{3+}:Citrate was used in the lowest ratio (1:1), as shown in assays 1 and 3 (Table A2, see Supplementary Material). The efficiency of this process increased when the molar ratio of Fe^{3+}:Citrate was

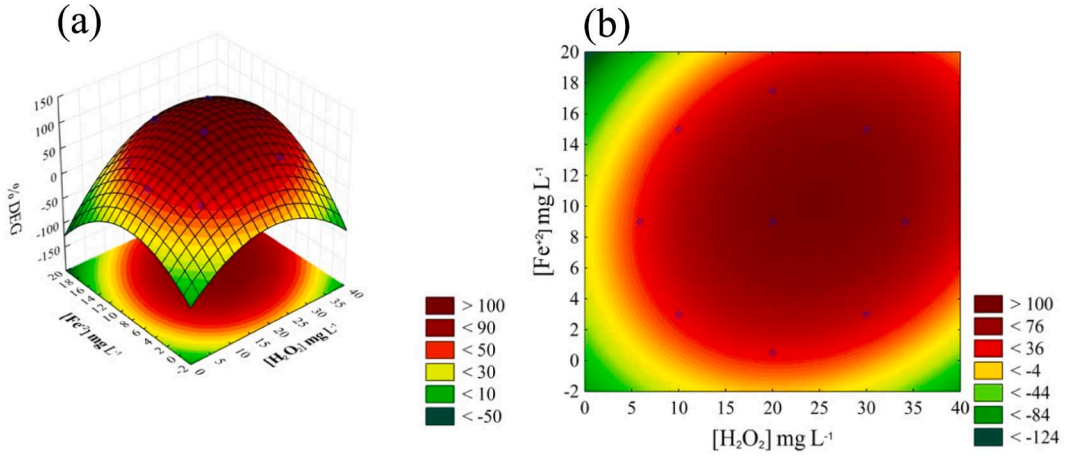

Fig. 6. Response surface graph (a) and contour curve (b) of the variables effects and their interactions on KET degradation.

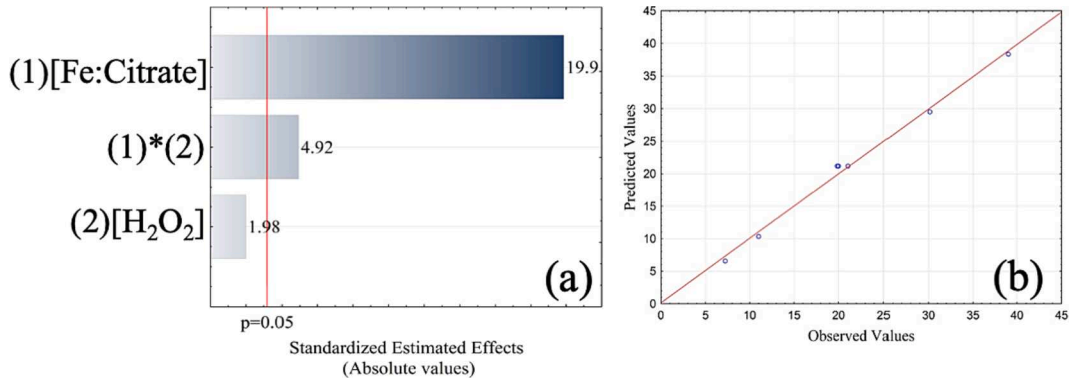

Fig. 7. (a) Pareto chart and (b) Predicted versus Observed Values for the variables effects and their interactions on percentage mineralization.

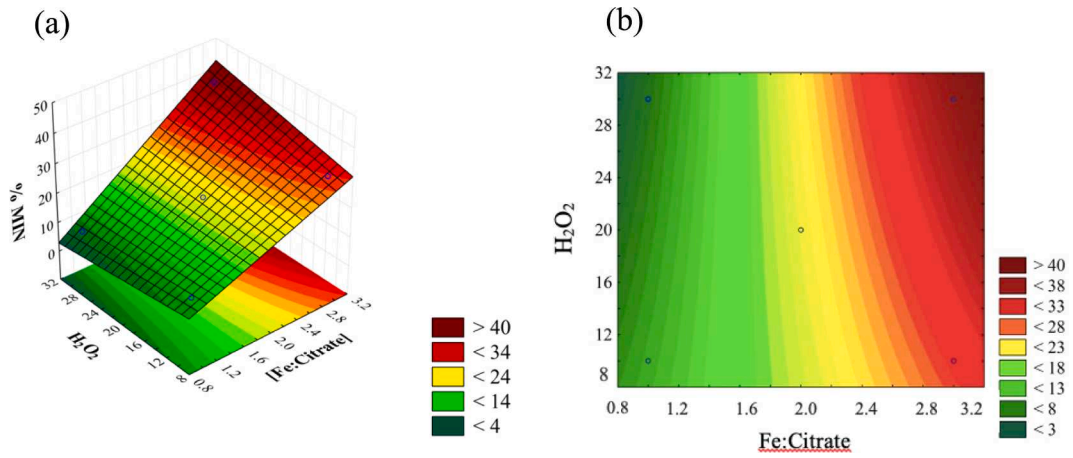

Fig. 8. Response surface graph (a) and contour curve (b) of the variables effects and their interactions on percentage mineralization.

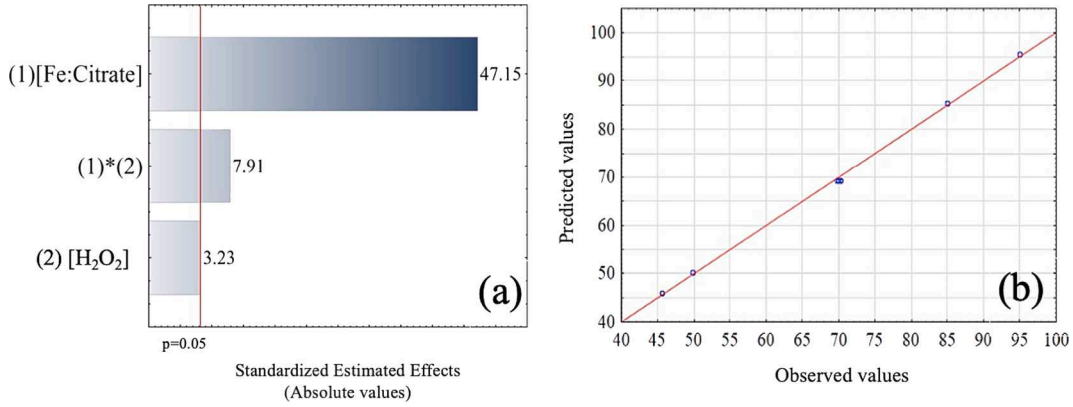

Fig. 9. Pareto chart (a) and Predicted vs. Observed Values (b) of the variables effects and their interactions on KET degradation.

adjusted to 1:3. These conditions prevented the precipitation of iron as iron hydroxides and avoided citrate competition for hydroxyl radicals [63]. The degradation of KET through the combined CW + SPF6 process in the presence of the ferric citrate complex can be attributed to the photoactivity of the Fe^{3+}:Citrate species, which generates Fe^{2+} with a relatively high quantum yield. At higher pH, the dominant species is $O_2^{\bullet -}$, favoring the formation of H_2O_2 and consequently HO•. Therefore, the optimized conditions were as follows: Fe^{3+}:Citrate (1:3); $[H_2O_2]$ = 30 mg L^{-1}; SRD_{UV} = 56.97 W m^{-2}; Q_{uv} = 3.69 kJ_{uv} L^{-1}; pH = 6.0 for a 120 min experiment.

Solar radiation in the photo-Fenton reaction has been used to increase the percentage of degradation of organic compounds [64–66]. In Table 2, some studies that used combined systems with solar photo-Fenton are selected.

Studies at pH levels below 5 (classic photo-Fenton) conducted by researchers [66–68] (Table 2) employed combined photo-Fenton systems. In the study carried out by [68], the combination was accomplished with a nanofiltration step, whereas [66] and [67] used immobilized biomass reactors (IBR). The study [67] is noteworthy for demonstrating the application of classic photo-Fenton (pH 2.6——2.8) combined with IBR for the removal of nalidixic acid (NDX) from industrial effluent. The authors achieved 100% degradation of NDX within 190 min and 90% mineralization within 400 min. The pH adjustment and time led to additional costs due to the need for chemical reagents to

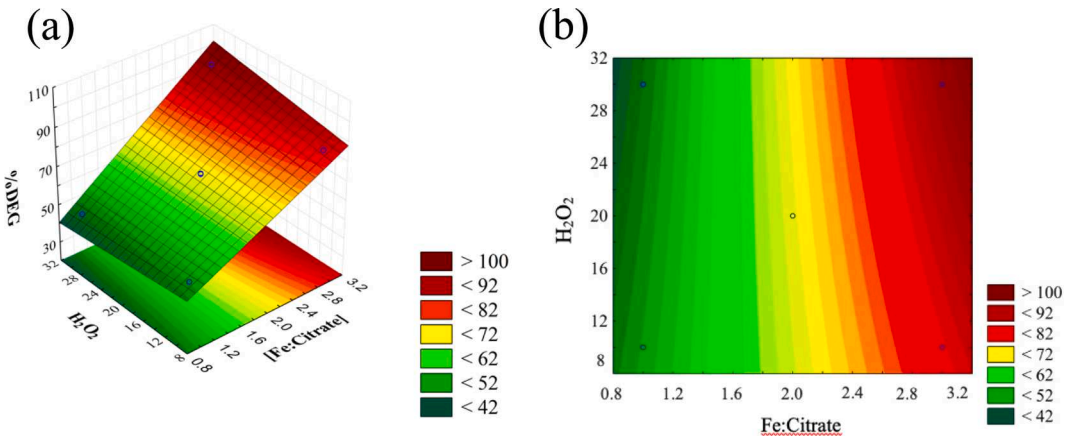

Fig. 10. Response surface graph (a) and contour curve (b) of the variables effects and their interactions on KET degradation.

first adjust the pH to acidic values and subsequently correct it to neutrality. Furthermore, it is important to observe that the amount of iron ion (Fe^{2+}, 20 mg L^{-1}) utilized in this study [67] significantly exceeded the disposal limits set by regulations, resulting in extra costs for pollutant removal. In our study, the allowed limits of Fe^{2+} as defined by regulations were adhered to. Moreover, the effluent's pH is close to neutral, without the need for prior pH correction, which translates to lower effluent treatment expenses. Other studies, such as [34] and [70], also achieved high degradation rates under nearly neutral conditions and pH 5–6, respectively, using the chelating agent EDDS for iron. Although EDDS is highly effective as a metal chelator, it is a synthetic compound not produced on a large scale, non-biodegradable, and expensive. Sodium citrate, employed in this research, is considered sustainable, has reduced cost, and is biodegradable, obtainable from natural sources like citrus fruits. In the study [22], it was not clear how the researchers managed to prevent iron precipitation while working at the natural effluent pH without the addition of chelating agents. It is essential to mention that this study [22] was conducted on a laboratory scale.

Our study stands out among the other studies in Table 2, as it is the only one that employed a combined system of constructed wetlands and solar photo-Fenton at a real scale, at near-neutral pH, with efficient removal of the pharmaceutical compound Ketoprofen, in a shorter experimental time, and with lower accumulated energy (Q_{uv}). Additionally, the optimization through experimental design, the assessment of physicochemical parameters, and the evaluation of toxicity in two bioindicators also differentiate this work from previously published studies, providing greater reliability in the results obtained for the potential reuse of the treated effluent.

The toxicity studies carried out by the authors highlighted in Table 2 were not carried out in Artemia sp. and Lactuca sativa, which were the focus of our work. In our study, these bioindicators did not indicate toxicity for the effluents treated after the combined CW + SPF6 process.

Among the studies presented in Table 2, this research focused on conducting of environmentally sustainable advanced solar oxidation processes combined with constructed wetlands, which are Nature-Based Solutions (NBS). This encompassed the selection of biodegradable and cost-effective reagents, as well as quantities within the limits established by Brazilian regulations and near neutral pH, resulting in a treated effluent free of toxicity and with physicochemical characteristics suitable for reuse. This initiative introduces the nexus concept and contributes to the implementation of circular economy principles.

3.2. Performance of the combined systems in the removal of physicochemical parameters

The combined constructed wetlands and solar photo-Fenton at pH 3.0 (CW + SPF3) and combined constructed wetlands and solar photo-Fenton at pH 6.0 (CW + SPF6) combined systems were effective in improving the physicochemical parameters of the treated effluents (Table 3). The removal performance of chemical oxygen demand (COD) (86.0% for both treatments), biochemical oxygen demand (BOD) (98% and 97% for CW + SPF3 and CW + SPF6, respectively), and turbidity (73.5% and 84.0% for CW + SPF3 and CW + SPF6, respectively) complied with current Brazilian legislation [72,73], and the combined systems were more efficient when compared to the individual systems (44% COD removal, 24% BOD removal, and 75% turbidity removal).

Combined systems have been used to enhance the efficiency of conventional treatment processes and advanced oxidation processes [74–76]. Table 3 presents the results of the physicochemical analyzes of the studied effluents.

3.3. Acute toxicity in Lactuca sativa

Based on the count of germinated seeds and measurements of radicle growth, the Germination Index (GI %), Effective Concentration (EC_{50}), and Toxic Unit (TU) [77,78] were calculated (Table A5, see Supplementary material).

The effluent treated by the CW + SPF6 process showed a GI value above 80%, indicating the absence of phytotoxic substances. All other samples had GI values below 80%, indicating some level of phytotoxicity in Lactuca sativa [78,79]. The GI value of CW + UV (52 ± 1.7 %), considered the blank in this study, did not show a significant difference compared to the effluent treated only by VFCW (49 ± 0.8 %).

The combined treatments CW + SPF3 and CW + SPF6 showed significant reductions in phytotoxicity, and the CW + SPF6 treatment was more efficient in increasing the germination index (%GI) with a difference of<20% between the treatment and control, indicating the absence of toxic characteristics for Lactuca sativa [52]. These results showed that no phytotoxic byproducts were generated for Lactuca sativa.

3.4. Acute toxicity in Artemia sp

Acute toxicity testing is usually the first step in toxicity investigation. Cysts of the microcrustacean Artemia sp. have been widely used because they are easy to handle and exhibit an acute toxicity response to persistent pollutants [80]. Toxicity results complement the physicochemical analyses and provide information on treatment performance [81,82].

The combined processes reduced the toxicity of the influent wastewater in the CW, with CW + SPF6 being more efficient in removing toxic substances, reducing the initial toxicity by 78.90% (Table A6, see Supplementary material) and making the effluent non-toxic (TU < 0.4). The effluent treated by CW + SPF3 exhibited moderate toxicity (TU between

Table 2
Research on the degradation of pharmaceutical contaminants by systems combined with solar photo-Fenton process.

Systems	Pharmaceutical contaminants	Aqueous matrix	Experimental conditions	Best toxicity results	Best degradation results	Total costs (U$ m^{-3})	Ref.
Solar photo Fenton combined with immobilized biomass reactor (IBR)	KET	Municipal wastewater	[KET] = 539 – 1090 ng/L [H_2O_2] = 60 mg/L; [Fe^{2+}] = 10 mg/L Q_{uv} = 4 kJ/L pH = 2.8	Not evaluated	95%	Not evaluated	[67]
Solar photo-Fenton process combined with IBR	NDX	Industrial wastewater	[NDX] = 45 mg/L [H_2O_2] = 72 mM; [Fe^{2+}] = 20 mg/L SRDuv = 30 W m^{-2} 190 min pH = 2.6 – 2.8	No toxicity for Daphnia magna and Vibrio fisheri	100%	Not evaluated	[68]
Solar photo Fenton combined with nanofiltration	KET	Municipal wastewater	[KET] = 160 ng/L and 740 – 800 ng/L [H_2O_2] = 50 mg/L; [Fe^{2+}] = 0.1 and 0.2 mM [Fe: EDDS] = 1:2 (molar ratio) pH = near neutral	high toxicity for Vibrio fisheri and Daphnia magna	90%	1.28	[34]
Solar photo Fenton combined with adsorption processes	FLU	Hospital wastewater	[FLU] = 500 µg/L e 5 mg/L [Fe^{2+}] = 5 mg/L [H_2O_2] = 50 mg/L pH = 5	Not evaluated	58%	Not evaluated	[69]
Solar photo-Fenton oxidation followed by adsorption on granular activated carbon (GAC)	Mixture of the antibiotics: AMP. CRT. ETM. OFX. SMX. TTC and TMP	Urban wastewater	[each antibiotic] = 100 µg L^{-1}; [Fe^{2+}] = 5 mg L^{-1}; [H_2O_2] = 50–100 mg L^{-1} pH = 2.8–2.9; [GAC] = 500 mg L^{-1}; contact time = 15 min pH = 7.5–8.0	No toxicity for Sorghum saccharatum, Lepidium sativum and Sinapis alba, and Daphnia magna	95%	Not evaluated	[70]
nanofiltration combined with (solar photo-Fenton. photo-Fenton-like Fe(III)–EDDS complex and ozonation	CBZ. FMQ. IBF. OFX and SMX	Natural water	[each pharmaceutical] = 15 µg L^{-1} [H_2O_2] = 25 mg/L [Fe: EDDS = 1:2 in mol Q_{uv} = 4.8 kJ/L SRDuv = 30 W m^{-2} pH = 5 – 6	Not evaluated	95% of the sum of drugs were degraded	Not evaluated	[71]
Horizontal constructed wetland – Solar Photo Fenton coupled system (laboratory scale)	DCF CBZ	CW effluent	[DCF; CBZ] = 15 µg/L [Fe^{2+}] = 5 mg/L [H_2O_2] = 50 mg/L SRDuv = 33.27 (±7.13) W/m^{-2}; 180 min pH = natural (7.2–7.3)	Not evaluated	92% 86%	Not evaluated	[22]
VFCW + Solar photo Fenton combined system (real scale)	KET	Anaerobic effluent post-treated by UASB reactor from Sewage Treatment Plant	[KET] = 25 mg/L [H_2O_2] = 30 mg/L [Fe: citrate] = 1:3 (molar ratio) Q_{uv} = 3.69 ± 0.11 kJ_{uv} L^{-1} SRD_{UV} = 56.97 (±1.66) W/m^{-2}; 120 min pH = near neutral	No toxicity for Artemia sp. and Lactuca sativa	95%	1.80	This work

0.4 and 1.0), removing 61.50% of the initial toxicity. Only the CW + UV process was not sufficient to remove toxicity, as it increased the toxicity of the effluent, indicating that UV radiation generated more toxic substances than those initially present [37,38]. These results are in accordance with [83], which demonstrated a decrease in effluent toxicity when the photo-Fenton process was applied. Another study that used solar photo-Fenton reaction at neutral pH with a ferric citrate complex in a 1:3 ratio showed toxicity reduction, making the effluent non-toxic and highlighting that the ferric citrate complex did not add toxicity to the effluent [84].

3.5. Cost analysis

There are many variables to consider for a cost study, and operational cost is one of the most common evaluations for comparing technology costs. Although the calculation of operational costs takes into account personnel, maintenance, electricity, materials, and services, in this study, the cost analysis was based only on the effluent treatment process using the performed processes. Therefore, only the consumption of electricity and chemical inputs used in each system was considered [75]. The results are presented in Table 4, considering the consumption

Table 3
Physicochemical characteristics of the effluent with 25 mg/L of KET before and after treatments by CW + SPF.

Samples	pH	Conductivity (mS cm^{-1})	Turbidity (NTU)	COD (mg/L)	BOD (mg/L)	Mineralization (%)	Degradation (%)	Efficiency (%) Turbidity	COD	BOD
Influent	7.7 ± 0.25	0.48 ± 0.04	28.50 ± 12.01	229.5 ± 6.80	95 ± 2.20	–	–	–	–	–
CW										
VFCW	5.6 ± 0.42	0.69 ± 0.02	7.20 ± 1.23	128.0 ± 11.31	72.5 ± 1.10	–	–	74.7	44.2	23.7
Photolysis	6.0	0.79 ± 0.05	15.01 ± 0.23	96.0 ± 6.36	12.5 ± 0.35	9.7 ± 0.015	53.5 ± 0.042	47.3	58.2	86.8
CW + SPF3	3.0	1.42 ± 0.16	7.54 ± 0.09	32.0 ± 2.24	2.0 ± 0.15	35.9 ± 1.31	96.6 ± 0.58	73.5	86.1	97.9
CW + SPF6	6.0	0.61 ± 0.04	4.56 ± 0.17	32.0 ± 1.82	2.9 ± 0.28	39.0 ± 0.65	95.0 ± 0.20	84.0	86.1	96.9

COD = Chemical Oxygen Demand; BOD = Biochemical Oxygen Demand; (±) standard deviation; (n = 3) triplicate analysis.

Table 4
Estimates of electrical and chemical costs for the treatments.

Treatment	Electrical cost* (U$/$m^3$)	Chemical cost (U$/$m^3$)	Total cost (U$/$m^3$)
CW + SPF3	0.064	2.27	2.33
CW + SPF6	0.064	1.74	1.80

*Electricity tariff in Campo Grande-MS, Brazil, July/2023: U$ 0.23 kWh.

per 1 m^3 of effluent treated.

Comparing this study with [34] research (Table 2), which focuses on a solar photo Fenton combined with nanofiltration system, we note that the treatment cost was stands at $1.28 per cubic meter, a figure lower than the $1.80 we obtained in this research. Nevertheless, the solar photo Fenton combined with nanofiltration approach detailed in [34] fell short in neutralizing the effluent's toxicity. Conversely, CW + SPF6 system not only effectively eliminated the toxicity but also curtailed the physicochemical parameters to levels suitable for effluent reuse, in accordance with Brazilian regulations.

4. Conclusions

The combined systems used (CW + SPF3 and CW + SPF6) achieved an average efficiency for KET degradation above 95%, while the standalone wetland unit achieved removal of 75% of the pharmaceutical. CW + SPF6 (with Citrate ligand) proves to be more advantageous, mainly because Brazilian legislation allows the discharge of effluents with a pH between 5 and 9, eliminating the need for a post-treatment neutralization step, which considerably reduces treatment costs.

The CW + SPF6 system showed a high capacity for the removal of conventional contaminants such as COD (86.1%), BOD (96.9%), and Turbidity (84%), resulting in concentrations of 32 mg L^{-1}, 2.9 mg L^{-1}, and 4.56 NTU, respectively, in the final effluent. It also reduced the toxicity (TU < 0.4) for Artemia sp. and Lactuca sativa.

Therefore, we recommend the use of the combined CW + SPF process, using Fe^{3+}:Citrate at a molar ratio of 1:3, 30 mg L^{-1} of H_2O_2, pH = 6.0, $SRD_{UV} = 56.97 \pm 1.66$ W m^{-2}, flow rate of 180 L min^{-1}, $Q_{uv} = 3.69 \pm 0.11$ kJ_{uv} L^{-1} for the treatment of anaerobic effluent from UASB reactors.

The solar photo-Fenton process and constructed wetlands are compatible methods, and their combination results in an innovative, effective, economically viable, and practical method for treating effluents contaminated with emerging pollutants. However, studies in a real scale, as presented here, are still lacking. Therefore, Nature-Based Solutions combined with advanced technologies are promising methods for the treatment and reuse of water in cities, providing several benefits, synergies, and cost opportunities in their entirety.

Declaration of Competing Interest

The authors declare that they have no known competing financial interests or personal relationships that could have appeared to influence the work reported in this paper.

Data availability

Data will be made available on request.

Acknowledgments

The authors wish to thank the Brazilian funding agencies Conselho Nacional de Desenvolvimento Científico e Tecnológico (CNPq), Coordenação de Aperfeiçoamento de Pessoal de Nível Superior (CAPES - Financing Code 001), and Fundação de Apoio ao Desenvolvimento do Ensino, Ciência e Tecnologia do Estado de Mato Grosso do Sul (FUNDECT).

Appendix A. Supplementary data

Supplementary data to this article can be found online at https://doi.org/10.1016/j.cej.2023.146282.

References

[1] M. Puri, K. Gandhi, M.S. Kumar, Emerging environmental contaminants: a global perspective on policies and regulations, J. Environ. Manage. 332 (2023), 117344, https://doi.org/10.1016/j.jenvman.2023.117344.
[2] A. Thresher, R. Foster, D.J. Ponting, S.A. Stalford, R.E. Tennant, R. Thomas, Are all nitrosamines concerning? A review of mutagenicity and carcinogenicity data, Regulatory Toxicology and Pharmacology. 116 (2020), 104749, https://doi.org/10.1016/J.YRTPH.2020.104749.
[3] S. Whitmee, A. Haines, C. Beyrer, F. Boltz, A.G. Capon, B. Ferreira, S. Dias, A. Ezeh, H. Frumkin, P. Gong, P. Head, R. Horton, G.M. Mace, R. Marten, S.S. Myers, S. Nishtar, S.A. Osofsky, S.K. Pattanayak, M.J. Pongsiri, C. Romanelli, A. Soucat, J. Vega, D. Yach, J. Pongsiri, The lancet commissions the rockefeller foundation-lancet commission on planetary health safeguarding human health in the anthropocene epoch: report of the rockefeller foundation-lancet commission on planetary health the lancet commissions, Lancet 386 (2015) 1973–2028, https://doi.org/10.1016/S0140-6736(15)60901-1.
[4] L. Hykrdová, O. Bajt, J. Jirkovský, Mechanism and kinetics of photochemical transformation of ketoprofen and its degradation intermediates, J. Hazard. Mater. 353 (2018) 70–79, https://doi.org/10.1016/J.JHAZMAT.2018.03.048.
[5] Y. Praveenkumarreddy, K. Vimalkumar, B.R. Ramaswamy, V. Kumar, R.K. Singhal, H. Basu, C.M. Gopal, K.E. Vandana, K. Bhat, H.N. Udayashankar, K. Balakrishna, Assessment of non-steroidal anti-inflammatory drugs from selected wastewater treatment plants of Southwestern India, Emerg Contam. 7 (2021) 43–51, https://doi.org/10.1016/J.EMCON.2021.01.001.
[6] L. Yin, B. Wang, H. Yuan, S. Deng, J. Huang, Y. Wang, G. Yu, Pay special attention to the transformation products of PPCPs in environment, Emerg Contam. 3 (2017) 69–75, https://doi.org/10.1016/J.EMCON.2017.04.001.
[7] E. Brillas, A review on the photoelectro-Fenton process as efficient electrochemical advanced oxidation for wastewater remediation. Treatment with UV light, sunlight, and coupling with conventional and other photo-assisted advanced technologies, Chemosphere. 250 (2020), 126198, https://doi.org/10.1016/j.chemosphere.2020.126198.
[8] I. Oller, S. Malato, Photo-Fenton applied to the removal of pharmaceutical and other pollutants of emerging concern, Curr. Opin. Green Sustain Chem. 29 (2021), 100458, https://doi.org/10.1016/j.cogsc.2021.100458.
[9] N. Özengin, A. Elmaci, Removal of pharmaceutical products in a constructed wetland, Iran J. Biotechnol. 14 (2016) 221–229. https://doi.org/10.15171/ijb.1223.
[10] Y. Zhang, M. Zhou, A critical review of the application of chelating agents to enable Fenton and Fenton-like reactions at high pH values, J. Hazard. Mater. 362 (2019) 436–450, https://doi.org/10.1016/j.jhazmat.2018.09.035.

[11] M. von Sperling, P.H. Sezerino, Dimensionamento De Wetlands Construídos No Brasil, Boletim Wetlands Brasil, Documento De Consenso Entre Pesquisadores E Praticantes, 2018, p. 65.

[12] M. Verduzo Garibay, A. Fernández del Castillo, J. de Anda, C. Senés-Guerrero, M. S. Gradilla-Hernández, Structure and activity of microbial communities in response to environmental, operational, and design factors in constructed wetlands, Int. J. Environ. Sci. Technol. 19 (2022) 11587–11612, https://doi.org/10.1007/s13762-021-03719-y.

[13] V.B. Santos, B.S. Machado, A. Atalla, P.S. Cavalheri, F.J.C. Magalhães Filho, Microbiological evaluation of constructed wetlands and solar disinfection in wastewater treatment and reuse, J. Water Health 18 (2020) 1146–1153, https://doi.org/10.2166/wh.2020.301.

[14] D.R. Manenti, P.A. Soares, A.N. Módenes, F.R. Espinoza-Quiñones, R.A. R. Boaventura, R. Bergamasco, V.J.P. Vilar, Insights into solar photo-Fenton process using iron(III)–organic ligand complexes applied to real textile wastewater treatment, Chem. Eng. J. 266 (2015) 203–212, https://doi.org/10.1016/J.CEJ.2014.12.077.

[15] N. de, M. Costa-Serge, R.G. Lima Gonçalves, M.A. Ramirez-Ubillus, C. Li, P. Hammer, S. Chiron, R.F. Pupo Nogueira, Effect of the interlamellar anion on CuMgFe-LDH in solar photo-Fenton and Fenton-like degradation of the anticancer drug 5-fluorouracil, Appl. Catal. B 315 (2022), 121537, https://doi.org/10.1016/J.APCATB.2022.121537.

[16] O. Gomes Júnior, M.G.B. Santos, A.B.S. Nossol, M.C.V.M. Starling, A.G. Trovó, Decontamination and toxicity removal of an industrial effluent containing pesticides via multistage treatment: coagulation-flocculation-settling and photo-Fenton process, Process Saf. Environ. Prot. 147 (2021) 674–683, https://doi.org/10.1016/j.psep.2020.12.021.

[17] J. Goerck, D.B. Wolff, R.K. de Araújo, S.T. Decezaro, Eletrocoagulação como pós-tratamento do efluente de um *wetland* construído de escoamento vertical, Engenharia Sanitaria e Ambiental. 26 (2021) 113–121, https://doi.org/10.1590/S1413-415220190068.

[18] F.L. Ferreira De Jesus, A. Teixeira De Matos, M. Pimentel De Matos, Efficiency of horizontal subsurface flow constructed wetlands cultivated with grasses of different root systems, (2020). https://doi.org/10.2166/ws.2020.210.

[19] M. de Oliveira, A.A. Atalla, B.E.F. Frihling, P.S. Cavalheri, L. Migliolo, F.J.C. M. Filho, Ibuprofen and caffeine removal in vertical flow and free-floating macrophyte constructed wetlands with Heliconia rostrata and Eichornia crassipes, Chem. Eng. J. 373 (2019) 458–467, https://doi.org/10.1016/j.cej.2019.05.064.

[20] M. de Oliveira, B.E.F. Frihling, J. Velasques, F.J.C.M. Filho, P.S. Cavalheri, L. Migliolo, Pharmaceuticals residues and xenobiotics contaminants: occurrence, analytical techniques and sustainable alternatives for wastewater treatment, Sci. Total Environ. 705 (2020), 135568, https://doi.org/10.1016/j.scitotenv.2019.135568.

[21] X. Li, H. Shi, K. Li, L. Zhang, Combined process of biofiltration and ozone oxidation as an advanced treatment process for wastewater reuse, Front. Environ. Sci. Eng. 9 (2015) 1076–1083, https://doi.org/10.1007/s11783-015-0770-5.

[22] H.A. Casierra-Martinez, C.A. Madera-Parra, X.M. Vargas-Ramírez, A. Caselles-Osorio, W.A. Torres-López, Diclofenac and carbamazepine removal from domestic wastewater using a Constructed Wetland-Solar Photo-Fenton coupled system, Ecol. Eng. 153 (2020), 105699, https://doi.org/10.1016/j.ecoleng.2019.105699.

[23] D.D. Ramos, P.C.S. Bezerra, F.H. Quina, R.F. Dantas, G.A. Casagrande, S. C. Oliveira, M.R.S. Oliveira, L.C.S. Oliveira, V.S. Ferreira, S.L. Oliveira, A. Machulek, Synthesis and characterization of TiO_2 and TiO_2/Ag for use in photodegradation of methylviologen, with kinetic study by laser flash photolysis, Environ. Sci. Pollut. Res. 22 (2015) 774–783, https://doi.org/10.1007/s11356-014-2678-1.

[24] D.R.V. Guelfi, E. Brillas, F. Gozzi, A. Machulek, S.C. de Oliveira, I. Sirés, Influence of electrolysis conditions on the treatment of herbicide bentazon using artificial UVA radiation and sunlight. Identification of oxidation products, J. Environ. Manage. 231 (2019) 213–221, https://doi.org/10.1016/j.jenvman.2018.10.029.

[25] L.C. Friedrich, M.A. Mendes, V.O. Silva, C.L.P.S. Zanta, A. Machulek, F.H. Quina, Mechanistic implications of Zinc(II) ions on the degradation of phenol by the fenton reaction, J. Braz. Chem. Soc. 23 (2012) 1372–1377, https://doi.org/10.1590/S0103-50532012000700022.

[26] M.F. Murrieta, E. Brillas, J.L. Nava, I. Sirés, Solar photoelectro-Fenton-like process with anodically-generated HClO in a flow reactor: Norfloxacin as a pollutant with a particular structure, Sep. Purif. Technol. 308 (2023), 122893, https://doi.org/10.1016/J.SEPPUR.2022.122893.

[27] E. Brillas, A critical review on ibuprofen removal from synthetic waters, natural waters, and real wastewaters by advanced oxidation processes, Chemosphere 286 (2022), 131849, https://doi.org/10.1016/j.chemosphere.2021.131849.

[28] D.R.V. Guelfi, F. Gozzi, A. Machulek, I. Sirés, E. Brillas, S.C. de Oliveira, Degradation of herbicide S-metolachlor by electrochemical AOPs using a boron-doped diamond anode, Catal. Today 313 (2018) 182–188, https://doi.org/10.1016/j.cattod.2017.10.026.

[29] A.J. Luna, O. Chiavone-Filho, A. Machulek, J.E.F. de Moraes, C.A.O. Nascimento, Photo-Fenton oxidation of phenol and organochlorides (2,4-DCP and 2,4-D) in aqueous alkaline medium with high chloride concentration, J. Environ. Manage. 111 (2012) 10–17, https://doi.org/10.1016/j.jenvman.2012.06.014.

[30] F. Gozzi, I. Sirés, S.C. de Oliveira, A. Machulek, E. Brillas, Influence of chelation on the Fenton-based electrochemical degradation of herbicide tebuthiuron, Chemosphere 199 (2018) 709–717, https://doi.org/10.1016/J.CHEMOSPHERE.2018.02.060.

[31] M. Clara, V.M. Starling, E.P. Costa, F.A. Souza, E.C. Machado, J. Calábria De Araujo, C.C. Amorim, Persulfate mediated solar photo-Fenton aiming at wastewater treatment plant effluent improvement at neutral pH: emerging contaminant removal, disinfection, and elimination of antibiotic-resistant bacteria, Environ. Sci. Pollut. Res. 28 (2021) 17355–17368, https://doi.org/10.1007/s11356-020-11802-z/Published.

[32] L. Clarizia, D. Russo, I. Di Somma, R. Marotta, R. Andreozzi, Homogeneous photo-Fenton processes at near neutral pH: A review, Appl Catal B 209 (2017) 358–371, https://doi.org/10.1016/J.APCATB.2017.03.011.

[33] K. O'Dowd, S.C. Pillai, Photo-Fenton disinfection at near neutral pH: Process, parameter optimization and recent advances, J. Environ. Chem. Eng. 8 (2020), https://doi.org/10.1016/J.JECE.2020.104063.

[34] S. Miralles-Cuevas, I. Oller, A. Agüera, J.A. Sánchez Pérez, S. Malato, Strategies for reducing cost by using solar photo-Fenton treatment combined with nanofiltration to remove microcontaminants in real municipal effluents: Toxicity and economic assessment, Chem. Eng. J. 318 (2017) 161–170, https://doi.org/10.1016/j.cej.2016.06.031.

[35] G.D. Silva, E.O. Marson, L.L. Batista, C. Ueira-Vieira, M.C.V.M. Starling, A. G. Trovó, Contrasting the performance of photo-Fenton at neutral pH in the presence of different organic iron-complexes using hydrogen peroxide or persulfate as oxidants for naproxen degradation and removal of antimicrobial activity, Process Saf. Environ. Prot. 147 (2021) 798–807, https://doi.org/10.1016/j.psep.2021.01.005.

[36] R. Ameta, A.K. Chohadia, A. Jain, P.B. Punjabi, Fenton and Photo-Fenton Processes, Advanced Oxidation Processes for Wastewater Treatment: Emerging Green Chemical Technology. (2018) 49–87. https://doi.org/10.1016/B978-0-12-810499-6.00003-6.

[37] S.K. Alharbi, J. Kang, L.D. Nghiem, J.P. van de Merwe, F.D.L. Leusch, W.E. Price, Photolysis and UV/H_2O_2 of diclofenac, sulfamethoxazole, carbamazepine, and trimethoprim: Identification of their major degradation products by ESI–LC–MS and assessment of the toxicity of reaction mixtures, Process Saf. Environ. Prot. 112 (2017) 222–234, https://doi.org/10.1016/J.PSEP.2017.07.015.

[38] J. Li, L.Y. Ma, L.S. Li, L. Xu, Photodegradation kinetics, transformation, and toxicity prediction of ketoprofen, carprofen, and diclofenac acid in aqueous solutions, Environ. Toxicol. Chem. 36 (2017) 3232–3239, https://doi.org/10.1002/etc.3915.

[39] R.V. Busto, J. Roberts, C. Hunter, A. Escudero, K. Helwig, L.H.G. Coelho, Mechanistic and ecotoxicological studies of amoxicillin removal through anaerobic degradation systems, Ecotoxicol. Environ. Saf. 192 (2020), 110207, https://doi.org/10.1016/j.ecoenv.2020.110207.

[40] BRASIL. Conselho Estadual de Recursos Hídricos do de Mato Grosso do Sul (CERH/MS). BRASIL., Deliberação n° 52, de 18 de junho de 2018. Dispõe sobre o enquadramento dos corpos de águas superficiais em consonância com as diretrizes estabelecidas na DELIBERAÇÃO CECA/MS Nº 36, de 27 de junho de 2012. Diário Oficial Do Estado Do Mato Grosso Do Sul. (2018) 39.

[41] APHA;AWWA;WWE, Standard methods for the examination of water and wastewater, 22edn ed., 2012.

[42] O. Levenspiel, Engenharia das reações químicas, Editora Blucher, 2000.

[43] L. Metcalf, H. Eddy, Tratamento de Efluentes e Recuperação de Recursos - 5ed - Leonard Metcalf, Harrison P, Eddy - Google Livros, 2015.

[44] T.R. Headley, R.H. Kadlec, Conducting hydraulic tracer studies of constructed wetlands: a practical guide, Ecohydrol. Hydrobiol. 7 (2007) 269–282, https://doi.org/10.1016/S1642-3593(07)70110-6.

[45] G.J. Maranata, N.O. Surya, A.N. Hasanah, Optimising factors affecting solid phase extraction performances of molecular imprinted polymer as recent sample preparation technique, Heliyon. 7 (2021), e05934, https://doi.org/10.1016/j.heliyon.2021.e05934.

[46] P.R. dos Santos, M.E. de Oliveira Dourados, I. Sirés, E. Brillas, R.P. Cavalcante, P. S. Cavalheri, P.L. Paulo, D.R.V. Guelfi, S.C. de Oliveira, F. Gozzi, A. Machulek Junior, Greywater treatment by anodic oxidation, photoelectro-Fenton and solar photoelectro-Fenton processes: Influence of relevant parameters and toxicity evolution, Process Saf. Environ. Prot. 169 (2023) 879–895, https://doi.org/10.1016/j.psep.2022.11.058.

[47] F. Alcaide, G. Álvarez, D.R.V. Guelfi, E. Brillas, I. Sirés, A stable CoSP/MWCNTs air-diffusion cathode for the photoelectro-Fenton degradation of organic pollutants at pre-pilot scale, Chem. Eng. J. 379 (2020), 122417, https://doi.org/10.1016/J.CEJ.2019.122417.

[48] D.H. Funai, F. Didier, J. Giménez, S. Esplugas, P. Marco, A. Machulek, Photo-Fenton treatment of valproate under UVC, UVA and simulated solar radiation, J. Hazard. Mater. 323 (2017) 537–549, https://doi.org/10.1016/j.jhazmat.2016.06.034.

[49] P.R. Michael, D.E. Johnston, W. Moreno, A conversion guide: Solar irradiance and lux illuminance, Journal of Measurements in Engineering. 8 (2020) 153–166. https://doi.org/10.21595/jme.2020.21667.

[50] S. Das, A.J. Misra, A.P. Habeeb Rahman, B. Das, R. Jayabalan, A.J. Tamhankar, A. Mishra, C.S. Lundborg, S.K. Tripathy, Ag@SnO_2@ZnO core-shell nanocomposites assisted solar-photocatalysis downregulates multidrug resistance in Bacillus sp.: A catalytic approach to impede antibiotic resistance, Appl Catal B 259 (2019), 118065, https://doi.org/10.1016/J.APCATB.2019.118065.

[51] D.C. Napoleão, L.E. Mendes Carneiro Zaidan, J.M. Rodríguez-Díaz, R.M. da Rocha Santana, M.C. Branco da Silva de Mendonça Montenegro, A. da Nova Araújo, M. Benachour, V. Lins da Silva, Use of the photo-Fenton process to discover the degradation of drugs present in water from the Wastewater Treatment Plants of the pharmaceutical industry, Afinidad. 75 (2018) 23–31.

[52] M.G. Bagur-González, C. Estepa-Molina, F. Martín-Peinado, S. Morales-Ruano, Toxicity assessment using Lactuca sativa L. bioassay of the metal(loid)s As, Cu, Mn, Pb and Zn in soluble-in-water saturated soil extracts from an abandoned mining site, J. Soil. Sediment. 11 (2011) 281–289, https://doi.org/10.1007/s11368-010-0285-4.

[53] G. Persoone, B. Marsalek, I. Blinova, A. Törökne, D. Zarina, L. Manusadzianas, G. Nalecz-Jawecki, L. Tofan, N. Stepanova, L. Tothova, B. Kolar, A practical and user-friendly toxicity classification system with microbiotests for natural waters and wastewaters, Environ. Toxicol. 18 (2003) 395–402, https://doi.org/10.1002/tox.10141.

[54] B. Lopez-Alvarez, R.A. Torres-Palma, F. Ferraro, G. Peñuela, Solar photo-Fenton treatment of carbofuran: Analysis of mineralization, toxicity, and organic by-products, J. Environ. Sci. Health A Tox. Hazard. Subst. Environ. Eng. 47 (2012) 2141–2150, https://doi.org/10.1080/10934529.2012.696029.

[55] L. de Melo, R. da Silva, R. Pereira Cavalcante, F. Fabbro Cunha, R.F. Gozzi, S.C. de Dantas, A.M. Oliveira, Tolfenamic acid degradation by direct photolysis and the UV-ABC/H_2O_2 process: factorial design, kinetics, identification of intermediates, and toxicity evaluation, Science of the Total Environment. 573 (2016) 518–531, https://doi.org/10.1016/j.scitotenv.2016.08.139.

[56] M.B. Kasiri, A.R. Khataee, Photooxidative decolorization of two organic dyes with different chemical structures by UV/H_2O_2 process: Experimental design, Desalination 270 (2011) 151–159, https://doi.org/10.1016/j.desal.2010.11.039.

[57] J.L. Wang, L.J. Xu, Advanced oxidation processes for wastewater treatment: Formation of hydroxyl radical and application, Crit. Rev. Environ. Sci. Technol. 42 (2012) 251–325, https://doi.org/10.1080/10643389.2010.507698.

[58] L. de Melo, F. da Silva, I. Gozzi, E. Sirés, S.C. de Brillas, A.M. Oliveira, Degradation of 4-aminoantipyrine by electro-oxidation with a boron-doped diamond anode: Optimization by central composite design, oxidation products and toxicity, Sci. Total Environ. 631–632 (2018) 1079–1088, https://doi.org/10.1016/J.SCITOTENV.2018.03.092.

[59] C.F. Bustillo-Lecompte, S. Ghafoori, M. Mehrvar, Photochemical degradation of an actual slaughterhouse wastewater by continuous UV/H_2O_2 photoreactor with recycle, J. Environ. Chem. Eng. 4 (2016) 719–732, https://doi.org/10.1016/j.jece.2015.12.009.

[60] A. Machulek, C. Vautier-Giongo, J.E.F. Moraes, C.A.O. Nascimento, F.H. Quina, Laser flash photolysis study of the photocatalytic step of the photo-fenton reaction in saline solution†, Photochem. Photobiol. 82 (2006) 208–212, https://doi.org/10.1562/2005-05-28-RA-548.

[61] D.R.V. Guelfi, Z. Ye, F. Gozzi, S.C. de Oliveira, A. Machulek Junior, E. Brillas, I. Sirés, Ensuring the overall combustion of herbicide metribuzin by electrochemical advanced oxidation processes. Study of operation variables, kinetics and degradation routes, Sep. Purif. Technol. 211 (2019) 637–645, https://doi.org/10.1016/J.SEPPUR.2018.10.029.

[62] C.P. Sharma, A. V Karim, A. Shriwastav, C. Prakash, S. Ansaf, V. Karim, Decolorization of methylene blue using Fe(III)-citrate complex in a solar photo-Fenton process: impact of solar variability on process optimization, (2019). https://doi.org/10.2166/wst.2019.411.

[63] A. De Luca, R.F. Dantas, S. Esplugas, Study of Fe(III)-NTA chelates stability for applicability in photo-Fenton at neutral pH, Appl Catal B 179 (2015) 372–379, https://doi.org/10.1016/J.APCATB.2015.05.025.

[64] A.J. Expósito, J.M. Monteagudo, I. Díaz, A. Durán, Photo-fenton degradation of a beverage industrial effluent: Intensification with persulfate and the study of radicals, Chem. Eng. J. 306 (2016) 1203–1211, https://doi.org/10.1016/J.CEJ.2016.08.048.

[65] N. Klamerth, S. Malato, M.I. Maldonado, A. Agüera, A.R. Fernández-Alba, Application of photo-fenton as a tertiary treatment of emerging contaminants in municipal wastewater, Environ. Sci. Tech. 44 (2010) 1792–1798, https://doi.org/10.1021/es903455p.

[66] D.H. Quiñones, P.M. Álvarez, A. Rey, S. Contreras, F.J. Beltrán, Application of solar photocatalytic ozonation for the degradation of emerging contaminants in water in a pilot plant, Chem. Eng. J. 260 (2015) 399–410, https://doi.org/10.1016/J.CEJ.2014.08.067.

[67] L. Prieto-Rodríguez, I. Oller, A. Agüera, S. Malato, Elimination of organic micro-contaminants in municipal wastewater by a combined immobilized biomass reactor and solar photo-Fenton tertiary treatment, J. Adv. Oxidation Technolo. 20 (2017), https://doi.org/10.1515/jaots-2016-0192.

[68] C. Sirtori, A. Zapata, I. Oller, W. Gernjak, A. Agüera, S. Malato, Decontamination industrial pharmaceutical wastewater by combining solar photo-Fenton and biological treatment, Water Res. 43 (2009) 661–668, https://doi.org/10.1016/j.watres.2008.11.013.

[69] A. Della-Flora, M.L. Wilde, P.S. Thue, D. Lima, E.C. Lima, C. Sirtori, Combination of solar photo-Fenton and adsorption process for removal of the anticancer drug Flutamide and its transformation products from hospital wastewater, J. Hazard. Mater. 396 (2020), 122699, https://doi.org/10.1016/j.jhazmat.2020.122699.

[70] S.G. Michael, I. Michael-Kordatou, V.G. Beretsou, T. Jäger, C. Michael, T. Schwartz, D. Fatta-Kassinos, Solar photo-Fenton oxidation followed by adsorption on activated carbon for the minimisation of antibiotic resistance determinants and toxicity present in urban wastewater, Appl Catal B 244 (2019) 871–880, https://doi.org/10.1016/j.apcatb.2018.12.030.

[71] S. Miralles-Cuevas, F. Audino, I. Oller, R. Sánchez-Moreno, J.A. Sánchez Pérez, S. Malato, Pharmaceuticals removal from natural water by nanofiltration combined with advanced tertiary treatments (solar photo-Fenton, photo-Fenton-like Fe(III)-EDDS complex and ozonation), Sep. Purif. Technol. 122 (2014) 515–522, https://doi.org/10.1016/j.seppur.2013.12.006.

[72] C.N. do M.A. Brasil, Dispõe sobre a classificação dos corpos de água e diretrizes ambientais para o seu enquadramento, bem como estabelece as condições e padrões de lançamento de efluentes, e dá outras providências, Resolução CONAMA nº 357/ 2005, Brasil, 2005.

[73] C.N. do M.A. Brasil, Dispõe sobre as condições e padrões de lançamento de efluentes, complementa e altera a Resolução no 357, de 17 de março de 2005, do Conselho Nacional do Meio Ambiente-CONAMA, Resolução CONAMA Nº 430, Brasil, 2011.

[74] M. Siddique, R. Farooq, G.J. Price, Synergistic effects of combining ultrasound with the Fenton process in the degradation of Reactive Blue 19, Ultrason. Sonochem. 21 (2014) 1206–1212, https://doi.org/10.1016/J.ULTSONCH.2013.12.016.

[75] D. da Silva, R. Pereira Cavalcante, E. Batista Barbosa, A. Machulek Junior, S. César de Oliveira, R.F. Dantas, Combined AOP/GAC/AOP systems for secondary effluent polishing: Optimization, toxicity and disinfection, Sep Purif Technol. 263 (2021).

[76] M.R. Granzoto, I. Seabra, J.A. Malvestiti, J. Cristale, R.F. Dantas, Integration of ozone, UV/H_2O_2 and GAC in a multi-barrier treatment for secondary effluent polishing: Reuse parameters and micropollutants removal, Sci. Total Environ. 759 (2021), 143498, https://doi.org/10.1016/j.scitotenv.2020.143498.

[77] M.C.; Sobrero, A.; Ronco, Ensayo de toxicidad aguda con semillas de lechuga Lactuca sativa L., in: IDRC, IMTA, 2004: pp. 55–67.

[78] Y.S. Aguerre, G.B. Gavazzo, Fitotoxicidad de papel reciclado. Ensayospreliminares, Proceedings of the ABTCP. (2012).

[79] P. Mañas, J. De las Heras, Phytotoxicity test applied to sewage sludge using Lactuca sativa L. and Lepidium sativum L. seeds, Int. J. Environ. Sci. Technol. 15 (2018) 273–280, https://doi.org/10.1007/S13762-017-1386-Z.

[80] D. Antonio da Silva, R.P. Cavalcante, R.F. Cunha, A. Machulek, S. César de Oliveira, Optimization of nimesulide oxidation via a UV-ABC/H_2O_2 treatment process: Degradation products, ecotoxicological effects, and their dependence on the water matrix, Chemosphere 207 (2018) 457–468, https://doi.org/10.1016/J.CHEMOSPHERE.2018.05.115.

[81] D. Movia, S. Bruni-Favier, A. Prina-Mello, In vitro alternatives to acute inhalation toxicity studies in animal models—a perspective, Front Bioeng. Biotechnol. 8 (2020) 1–10, https://doi.org/10.3389/fbioe.2020.00549.

[82] I. Pinto, S. Rodrigues, O.M. Lage, S.C. Antunes, Assessment of water quality in aguieira reservoir: ecotoxicological tools in addition to the water framework directive, Ecotoxicol. Environ. Saf. 208 (2021), 111583, https://doi.org/10.1016/J.ECOENV.2020.111583.

[83] M. Lapertot, S. Ebrahimi, S. Dazio, A. Rubinelli, C. Pulgarin, Photo-Fenton and biological integrated process for degradation of a mixture of pesticides, J. Photochem. Photobiol. A Chem. 186 (2007) 34–40, https://doi.org/10.1016/J.JPHOTOCHEM.2006.07.009.

[84] O. Gomes Júnior, L.L. Batista, C. Ueira-Vieira, R.M.F. Sousa, M.C.V.M. Starling, A. G. Trovó, Degradation mechanism of fipronil and its transformation products, matrix effects and toxicity during the solar/photo-Fenton process using ferric citrate complex, J. Environ. Manage. 269 (2020), 110756, https://doi.org/10.1016/j.jenvman.2020.110756.